

Separation mechanism in dehydration of water/organic binary liquids by pervaporation through microporous silica

J. Sekulić, J.E. ten Elshof*, D.H.A. Blank

*University of Twente, Inorganic Materials Science, MESA⁺ Institute of Nanotechnology and Faculty of Science and Technology,
P.O. Box 217, 7500 AE Enschede, The Netherlands*

Received 22 October 2004; received in revised form 9 January 2005; accepted 10 January 2005

Available online 17 February 2005

Abstract

The pervaporation properties of two microporous three-layer stacked ceramic membranes that differ only with respect to the nature of the mesoporous interlayer are discussed. The adsorption–diffusion model and Maxwell–Stefan theory are applied to explain the influence of process parameters on the pervaporation of selected binary liquids. The temperature, feed concentration and chemical nature of the permeating species were varied. The membrane system α -Al₂O₃/ γ -Al₂O₃/microporous SiO₂ was found to have the highest selectivity for dewatering of alcohols. This is due to a combination of small pores in the microporous silica layer, and the hydrophilicity of this layer. When γ -Al₂O₃ was replaced by mesoporous anatase, lower separation factors were obtained. The hydrophilicity of the silica top layer appears to be influenced by the nature of the underlying mesoporous supporting layer.

© 2005 Elsevier B.V. All rights reserved.

Keywords: Pervaporation; Adsorption–diffusion model; Membrane; Silica; Hydrophilicity

1. Introduction

Pervaporation and vapor permeation are separation technologies in which one of the components of a liquid mixture (pervaporation), or a vapor phase (vapor permeation) is separated from the feed mixture by selective evaporation (pervaporation) or gas transport (vapor permeation) through a membrane. In principle, these technologies have better separation capacity and energy efficiency than competing distillation, adsorption and extraction technologies and their application may lead to energy reductions of 40–60% [1]. However, the application of pervaporation/vapor permeation in the chemical industry has been restricted due to severe limitations of the current generation of commercially available membranes, i.e., their low chemical and thermal stability, insufficient selectivity and low flux [2–5].

Although ceramic membranes are virtually inert in non-aqueous organic solvents and offer high temperature

stability, they are not stable in aqueous corrosive liquids like strong acids and alkaline solutions [2–7]. Since ceramic membranes are commonly stacked layer systems, containing a macroporous support, a mesoporous intermediate layer and a microporous top layer, the stability of each layer may determine the stability of the complete system. α -Alumina is usually used as macroporous support, because of its good mechanical properties and high thermal and chemical stability [4]. The most commonly applied system α -alumina/ γ -alumina/silica is only stable in a narrow range of pH between 4 and 10. This is mainly due to the poor chemical stability of the γ -alumina phase. Replacing γ -alumina by crystalline mesoporous titania (anatase) improves the stability of the system considerably, especially in acidic environments, since the mesoporous titania/microporous silica system is stable in the pH range 0–10 [6–8].

An understanding of the transport and separation mechanisms is crucial for further development of a membrane pervaporation process in terms of choice of suitable membrane materials and adjustment of process parameters that lead to enhanced separation and higher fluxes. The separation factor

* Corresponding author. Tel.: +53 489 2695; fax: +31 53 489 4683.

E-mail address: j.e.tenelshof@utwente.nl (J.E. ten Elshof).

α of a membrane is generally defined as the ratio of concentrations of components i and j in the permeate relative to that in the feed:

$$\alpha = \frac{y_i/x_i}{y_j/x_j} \quad (1)$$

in which y and x are the fractions of components i and j in the permeate and feed, respectively.

The steps in a pervaporation process are sorption at the interface between the feed and the membrane, diffusion across the membrane due to concentration gradients (rate determining steps), and finally desorption into the vapor phase at the permeate side of the membrane. The first two steps are primarily responsible for the final permselectivity [9–11]. The solution–diffusion model is generally accepted as a good description of the mechanism of fluid transport, and is widely applied in the area of polymeric membrane research [10]. Applied to zeolite and ceramic membranes, it was renamed into the adsorption–diffusion model.

The Maxwell–Stefan theory is the most often used model to describe transport of binary mixtures through a membrane [12–17]. A description of pervaporation through ceramic microporous membranes in terms of the Maxwell–Stefan theory was given by Verkerk et al. [15]. Considering the one-dimensional transport of a mobile component i from a binary mixture composed of components i and j through a membrane M , the driving force of component i can be expressed in terms of the Maxwell–Stefan theory as [15]

$$-\frac{1}{p_i} \frac{dp_i}{dz} = \frac{x_j}{\mathcal{D}_{ij}} \left(\frac{J_i}{c_i} - \frac{J_j}{c_j} \right) + \frac{1}{\mathcal{D}'_{iM}} \frac{J_i}{c_i} \quad (2)$$

where p_i is the partial pressure of component i , J_i (J_j) and c_i (c_j) the flux and concentration of component i (j), respectively, z the direction of transport (perpendicular to the membrane surface area), x_j the molar fraction of component j , \mathcal{D}_{ij} the Maxwell–Stefan micropore diffusivity between components i and j , and \mathcal{D}'_{iM} the Maxwell–Stefan micropore diffusivity of component i in the membrane. An explicit expression for J_i can be obtained from Eq. (2) if J_j/c_j is negligible in comparison with J_i/c_i . It was shown that the flux of the majority component i can then be expressed as [16]

$$J_i = H_i \left(\frac{\bar{x}_j}{\mathcal{D}_{ij}} + \frac{1}{\mathcal{D}'_{iM}} \right)^{-1} \frac{\Delta p_i}{L} \quad (3)$$

where L is the thickness of the selective membrane layer, and $\Delta p_i = p_i^f - p_i^p$, with p_i^f and p_i^p the vapor partial pressures of component i at the feed and permeate side of the membrane, respectively. The simplifying assumption made here is that x_j , which is a function of position z , can be approximated by the average of the molar fractions on opposite sides of the membrane \bar{x}_j . The Henry coefficient H_i is the adsorption coefficient of component i on the membrane surface and depends on temperature according to [15]:

$$H_i = H_i^0 e^{Q_i/RT} \quad (4)$$

Here Q_i is the heat of adsorption of species i , H_i^0 a pre-exponential constant, R the gas constant, and T the temperature. The factor containing the Maxwell–Stefan diffusivities can be regarded as an effective diffusion coefficient $\mathcal{D}_i^{\text{eff}}$:

$$\mathcal{D}_i^{\text{eff}} = \left(\frac{\bar{x}_j}{\mathcal{D}_{ij}} + \frac{1}{\mathcal{D}'_{iM}} \right)^{-1} \quad (5)$$

In sufficiently small temperature intervals it may be approximated by an Arrhenius-type expression

$$\mathcal{D}_i^{\text{eff}} = \mathcal{D}_i^{\text{eff},0} e^{-E_i^{\text{D}}/RT} \quad (6)$$

where E_i^{D} and $\mathcal{D}_i^{\text{eff},0}$ are the apparent activation energy of diffusion and a pre-exponential constant, respectively. From Eqs. (3) and (5) the permeance F_i can be expressed as

$$F_i = \frac{J_i}{\Delta p_i} = \frac{H_i \mathcal{D}_i^{\text{eff}}}{L} \quad (7)$$

so that the activation energy of permeance E_i^{F} is $E_i^{\text{F}} = E_i^{\text{D}} - Q_i$.

In this paper, the pervaporation properties of microporous silica membranes are studied. The adsorption–diffusion model and Maxwell–Stefan theory are applied to explain the influence of process parameters on the pervaporation of selected binary liquids. The temperature, feed concentration and nature of the permeating species were varied. The aim was to get a better understanding of the separation mechanism in pervaporation, and also to study the influence of the underlying supporting layer on flux and separation properties of the microporous top layer.

2. Experimental

2.1. Membranes

The α -Al₂O₃ macroporous supports were made from α -alumina powder (AKP30, Sumimoto, Japan) by the colloidal filtration technique [18]. After sintering the supports were disc-shaped, with diameter 39 mm, thickness 2 mm, mean pore radius 100 nm, and porosity \sim 30%.

The mesoporous intermediate layer was either γ -Al₂O₃ (calcined at 600 °C), or based on the anatase phase of titania (calcined at 450 °C) [19,20]. In some experiments, the titania phase was doped with 5–20 mol% of zirconia and calcined at 450–700 °C. The intermediate layers were applied onto the α -Al₂O₃ discs by a dip-coating technique. After calcination, these layers had similar structural characteristics: a thickness of 1–2 μ m, pore sizes of 5–8 nm, and porosities of 40% (zirconia-doped titania) and 55% (γ -alumina).

Polymeric silica sols for microporous top layers were made by acid-catalysed hydrolysis and condensation of suitable alkoxides, as described in more detail elsewhere [21]. The sols were deposited onto the surface of the mesoporous layer by dip-coating. The silica membranes were calcined at

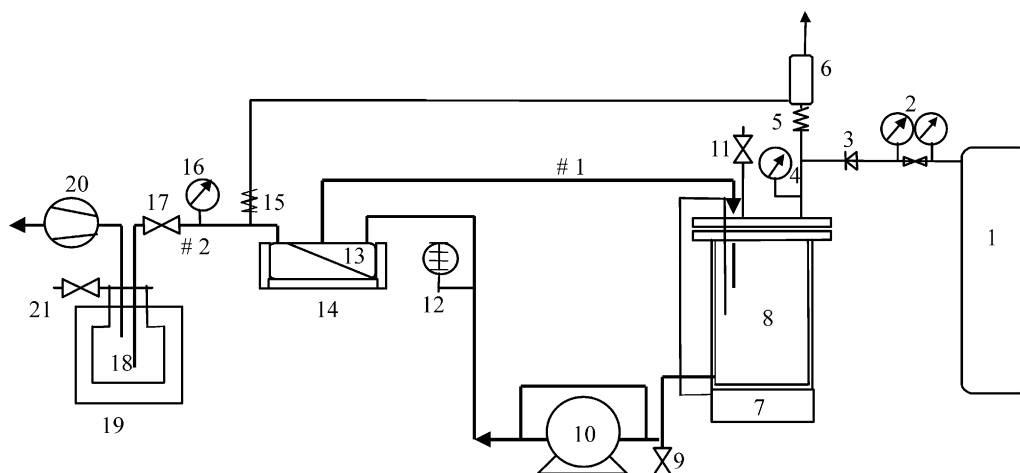


Fig. 1. Schematic diagram of pervaporation unit.

400 °C. The resulting layers were amorphous, with a thickness of ~100 nm and pore sizes in the range of 0.3–0.5 nm.

2.2. Pervaporation and gas separation experiments

Pervaporation experiments were carried out using a laboratory scale pervaporation unit (Fig. 1). The feed mixture, contained in a 2 l heated vessel (indicated by 8 in Fig. 1) under a pressure of 2–3 bar, was pumped continuously in the pulls mode (10) through the feed compartment of the pervaporation unit (14), where it came into direct contact with the top layer of the membrane (13). The retentate was recycled to the feed vessel (#1). The permeate side of the membranes was kept under near-vacuum (6–8 mbar) with a vacuum pump (20). Steady state fluxes were determined by collecting the permeate side vapors in an ethanol-based cold trap and measuring the weight increase with time (18). The feed and permeate compositions were determined by Karl Fischer titration (784 KFP Titrino, Metrohm, Switzerland).

The pervaporation experiments were performed in the temperature range 30–100 °C. The feed mixtures were binary liquids with 2–20 wt.% water (on total weight) in ethanol, 2-propanol, or 2-butanol (all obtained from Merck, Germany).

The partial vapor pressures at the feed side was calculated from $p_i^f = x_i \gamma_i p_i^0$, where x_i is the molar fraction of component i in the liquid phase, γ_i the activity coefficient, and p_i^0 the vapor pressure of pure component i at a given temperature. The values of γ_i were calculated with the Wilson equation, and p_i^0 using the Antoine equation [22]. The partial vapor pressures at the permeate side were calculated from the molar fractions in the permeate and the total pressure.

Gas separation experiments were performed with H₂/CH₄ feed mixtures at 200 °C in a cross-flow gas permeation setup as described elsewhere [23]. Prior to the permeation experiments the membranes were dried at 300 °C under a helium stream to remove any moisture from the pore structure. The membranes were placed in a stainless-steel cell with the mi-

croporous membrane top-layer at the feed side. The composition of the gas mixture at the feed side was controlled by mass flow controllers. The feed pressure and the pressure difference over the membrane were measured by electronic pressure transducers. Argon was used as sweep gas with a flow of 120 ml/min. The gas composition of permeate and retentate were analyzed by a gas chromatograph (Varian, Star 3400CX).

2.3. Characterization

NH₃ temperature programmed desorption (TPD) [24,25] was performed in order to determine the presence of acidic sites on the membrane pore surface. About 80 mg of the sample was activated at 400 °C for 1.5 h, then evacuated for 30 min, cooled to room temperature, and equilibrated with NH₃ at 50 °C, at a pressure of 7 mbar. The time for reaching the adsorption equilibrium was 60 min. The excess ammonia was evacuated from the sample. A temperature program was set from 50 to 650 °C with a heating rate of 10 °C/min. All data were calibrated with sample weight.

X-ray photoelectron spectroscopy (XPS, PHI Quantera Scanning ESCA Microprobe, USA) with Ar⁺ sputtering (sputter rate 5.1 nm/min; 2 keV Ar⁺) was carried out to identify the atomic concentrations of silica, alumina and titania by measuring the Si 2p, Al 2p and Ti 2p spectra as a function of depth inside the layer.

3. Results and discussion

3.1. Influence of process parameters

Fluxes and separation factors of titania-supported silica membranes in the separation of 2-butanol/water and 2-propanol/water mixtures are shown in Fig. 2. Separation factors up to 500 and 100, and total fluxes up to 1.7

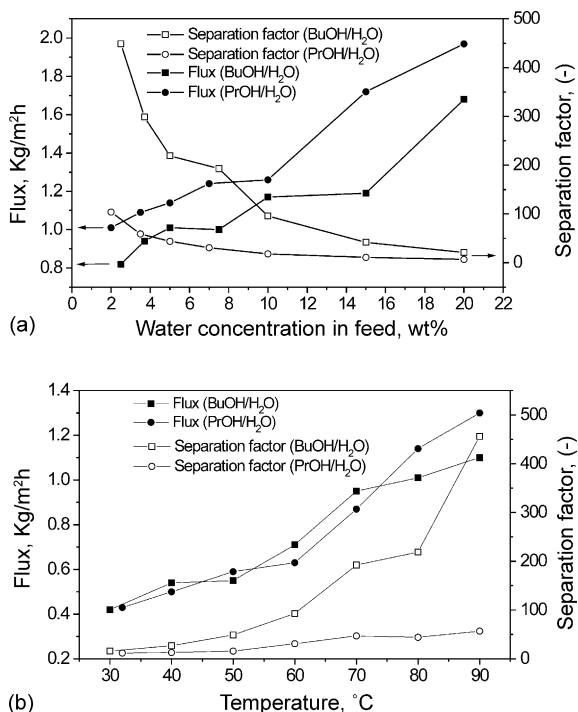


Fig. 2. Separation factors and total fluxes of an α -Al₂O₃/Zr-doped TiO₂/SiO₂ membrane as a function of (a) feed composition at 80 °C, and (b) temperature at a feed composition 5 wt.% H₂O/95 wt.% alcohol.

and 2.2 kg/m² h were measured for 2-butanol/water and 2-propanol/water, respectively. Experiments were also carried out with ethanol/water mixtures (not shown in the figure), where separation factors up to 20 and fluxes up to 1.3 kg/m² h were measured. In general, the membranes showed the highest separation factors and lowest fluxes for 2-butanol/water mixtures, followed by 2-propanol and ethanol/water mixtures. Since the average pore size of the silica membrane of 0.3–0.5 nm, and the molecular sizes of 2-butanol, 2-propanol, and ethanol are \sim 0.55, 0.5 and 0.45 nm, respectively, these selectivity differences can be explained by a separation mechanism based on size exclusion effects [11,16].

The total flux increased, while the separation factor decreased with increasing water content as shown in Fig. 2(a). The decrease in selectivity with increasing water content is often attributed to the so-called “drag” effect [15,16]. In terms of Maxwell–Stefan theory, the velocity of water is higher than the velocity of alcohol ($J_{\text{H}_2\text{O}}/c_{\text{H}_2\text{O}} > J_{\text{alcohol}}/c_{\text{alcohol}}$), so according to Eq. (2) the first term on the right hand side is negative, which implies that the alcohol flux is larger than expected on the basis of its own driving force.

Fig. 2(b) shows that both separation factor and flux increase with temperature for all studied mixtures, confirming an improved pervaporation performance at elevated temperatures [15]. In accordance with the adsorption–diffusion model, a higher flux is a consequence of an increased driving force due to the increased (virtual) vapor pressure of the components in the feed, but possibly also due to an increased mobility of the adsorbed species.

Table 1

Apparent activation energies of permeance E^F in the pervaporation of binary liquids with 10 wt.% water in the feed through titania-supported silica membrane

Binary liquid	E^F (kJ/mol)	
	Water	Alcohol
Water/2-butanol	3.8 ± 1.3	-15.6 ± 1.0
Water/2-propanol	2.9 ± 1.2	3.1 ± 1.0

The calculated activation energies of permeance $F_i = J_i/\Delta P_i$ of all components are listed in Table 1. The results are in agreement with the data of Verkerk et al. [15] and ten Elshof et al. [16], who also reported an activation energy of water permeance of around zero for a γ -alumina supported silica membrane.

The mass fluxes of components at 80 °C versus their partial pressure differences over the membrane are shown in Fig. 3. The water fluxes in Fig. 3(a) increased with partial pressure difference of water, confirming that the water flux is only dependent on its own driving force. However, the decreasing alcohol fluxes with increasing driving force clearly show that the dragging effect by water dominates the alcohol flux.

Since the fluxes of 2-propanol and 2-butanol are low compared to the water fluxes, and both organic solvents

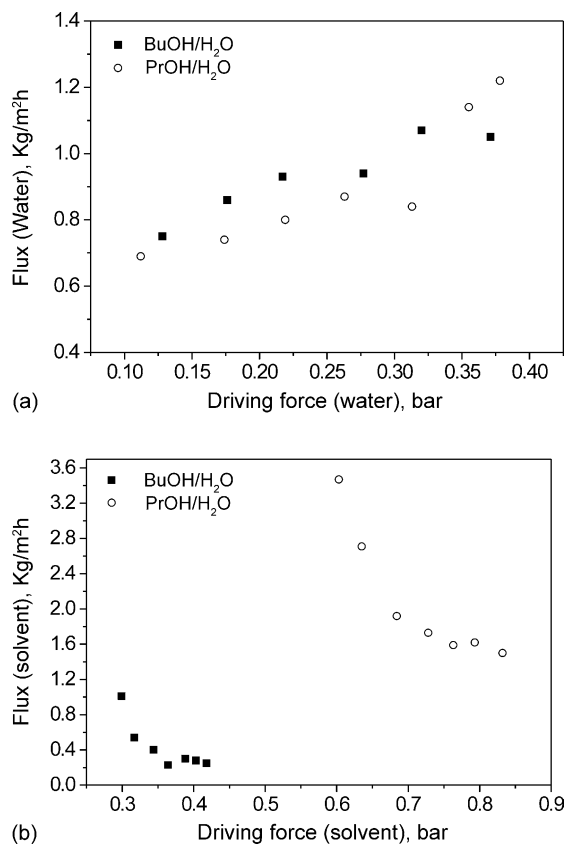


Fig. 3. Mass fluxes vs. partial vapor pressure difference across the membrane at 80 °C: (a) water fluxes and (b) corresponding alcohol fluxes.

Table 2
Estimated Maxwell–Stefan micropore diffusion coefficients

Binary liquid	$\mathcal{D}'_{\text{water,M}}$ (m ² /s)	$\mathcal{D}_{\text{water,alcohol}}$ (m ² /s)
Water/2-butanol	1.2×10^{-13}	6.3×10^{-15}
Water/2-propanol	1.0×10^{-13}	6.9×10^{-15}

are expected to adsorb considerably on silica, Eq. (3) can be used to estimate $\mathcal{D}'_{\text{water,M}}$ and the friction coefficients $\mathcal{D}_{\text{water,alcohol}}$. For the sake of simplicity it was assumed that the friction coefficients have constant values over the entire feed composition interval. Adopting $H_{\text{water}} = 3.8 \text{ mol/m}^3 \text{ Pa}$ from literature [15,16], good fits were obtained with the parameters listed in Table 2. The water diffusion coefficient $\mathcal{D}'_{\text{water,M}} = 1 \times 10^{-13} \text{ m}^2/\text{s}$ obtained from the fits is lower than the value reported by Verkerk et al., who estimated $\mathcal{D}'_{\text{water,M}} = 9 \times 10^{-13} \text{ m}^2/\text{s}$ for 2-propanol/water [15]. However, they assumed that H_{water} is $0.8 \text{ mol/m}^3 \text{ Pa}$, which leads to higher predicted values for $\mathcal{D}'_{\text{water,M}}$ than with a Henry coefficient of $3.8 \text{ mol/m}^3 \text{ Pa}$ as we used here. The same holds for the values of the friction coefficients ($\mathcal{D}_{\text{water,alcohol}} \sim 6\text{--}7 \times 10^{-15} \text{ m}^2/\text{s}$) of 2-propanol and 2-butanol, which are smaller than the reported friction coefficients of $0.8\text{--}2.0 \times 10^{-13} \text{ m}^2/\text{s}$ [15] for 2-propanol/water.

3.2. Influence of mesoporous intermediate layer

A selection of pervaporation data with various membranes and feed mixtures is shown in Table 3. These measurements were carried out at 80°C . High separation factors (800–1000) and reasonable fluxes were measured on γ -alumina supported silica membranes (experiments I and II). Surprisingly, the separation factors of the same separations decreased considerably when the intermediate layer material was changed from γ -alumina into mesoporous titania (experiments III and IV).

To examine the possible presence of defects that might explain the differences in membrane permselectivity during pervaporation, gas permeation experiments were carried out on γ -alumina and titania-supported silica membranes. At 200°C , the H_2 permeance F_{H_2} was in the range of $4\text{--}7 \times 10^{-7} \text{ mol/m}^2 \text{ s Pa}$, and the H_2/CH_4 permselectivity $F_{\text{H}_2}/F_{\text{CH}_4}$ of a 1:1 H_2/CH_4 gas mixture was ~ 50 for both types of membranes. Since the permselectivity of a membrane in gas separation is very sensitive to the presence

of mesopores and/or defects in the separation layer, the high permselectivities found here strongly suggest that both membranes were virtually defect-free. A certain difference in morphology of the top silica layer may still be possible due to possibly different layer thicknesses and different penetration depths of silica into the underlying mesoporous layer, but it can be concluded from the gas permeation data that the intermediate layers seem to have no substantial influence on the intrinsic membrane separation properties that are typically associated with a molecular size sieving mechanism.

Considering the fact that the main difference between the γ -alumina and titania membranes are the elemental compositions, it is possible that the surface properties play a definite role in the separation mechanism. The silica/alumina and silica/titania layers were therefore characterized by XPS analysis with depth profiling. From the “bulk” γ -alumina layer towards the SiO_2 surface, a clear shift in the Al 2p spectrum from 74 eV (the binding energy that corresponds to Al_2O_3) to 75.1 eV can be observed in Fig. 4(a) [26]. In the Si 2p spectrum, a binding energy peak shift from 103.2 (SiO_2) to 101.6 eV occurs. These shifts indicate the existence of compounds other than SiO_2 and Al_2O_3 in the interfacial region, for example Al_2OSiO_4 (corresponding binding energy of 74.8 eV in Al 2p spectra), $\text{Al}_4\text{Si}_4\text{O}_{10}(\text{OH})_8$ (102.6 eV in the Si 2p spectrum) [26], or related compounds. Although these examples represent crystalline materials, the presence of various silico-aluminate-like compounds suggests a chemical reaction between silica and γ -alumina in the interfacial region, leading to the incorporation of aluminum atoms into the silica matrix, and vice versa. Similar results were obtained by XPS analysis of the mesoporous titania/silica interface, shown in Fig. 4(b), which also showed the formation of a mixed element matrix. It is not entirely clear in which stage of the synthesis these layers are formed, but mutual penetration of silica into the underlying material (and vice versa) is evident.

Due to the trivalent nature of Al it is possible that acidic sites are formed when an aluminum atom is embedded in the amorphous silica matrix. This could make the silica layer more hydrophilic, so that the value of the Henry constant of water would increase (Eq. (3)). On the other hand, no increase of the number of acidic sites is expected when titanium is present in the silica matrix, since its oxidation state (4+) is the same as that of silica.

Table 3
Selected results of gas permeation and pervaporation experiments on microporous silica membranes with different mesoporous intermediate layers

Experiment	Intermediate layer	Gas permeation		Pervaporation		
		F_{H_2} (mol/m ² s Pa)	Permselectivity $F_{\text{H}_2}/F_{\text{CH}_4}$	Feed (wt./wt.)	Total flux (kg/m ² h)	Separation factor
I	$\gamma\text{-Al}_2\text{O}_3$	4.0×10^{-7}	50	90/10 EtOH/H ₂ O	1.0	8.0×10^2
II				95/5 2-BuOH/H ₂ O	1.0	1.0×10^3
III	TiO_2	7.2×10^{-7}	42	90/10 EtOH/H ₂ O	1.3	19
IV				95/5 2-BuOH/H ₂ O	0.6	2.2×10^2

Gas permeation and separation experiments were performed at 200°C . Pervaporation fluxes and separation factors at 80°C are reported.

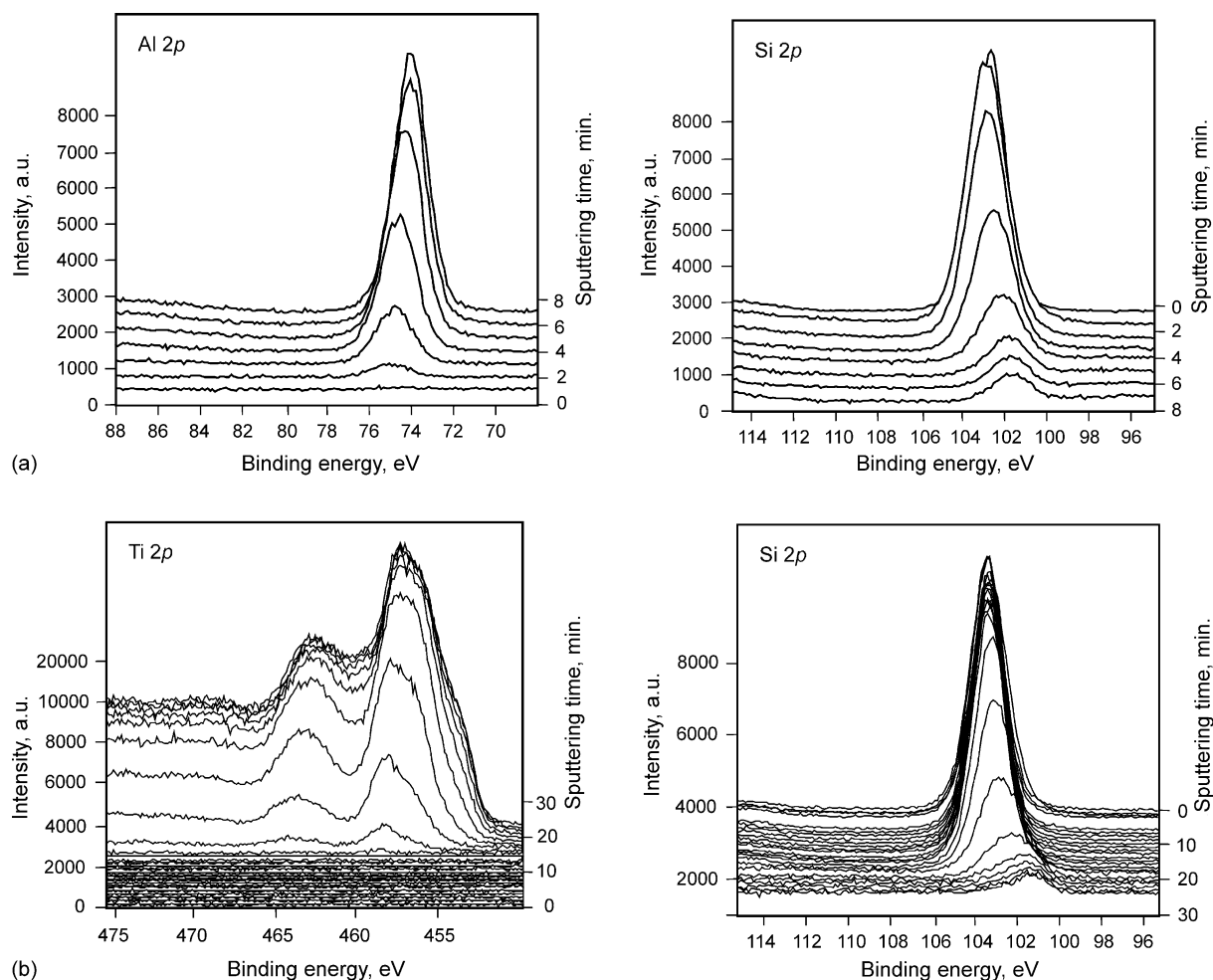


Fig. 4. XPS depth profile. (a) Al 2p and Si 2p spectra of the γ -alumina/silica interfacial region; (b) Ti 2p and Si 2p spectra of the titania/silica interfacial region.

The presence of acidic sites in the mixed alumina/silica material was verified by temperature programmed desorption (TPD) using NH_3 . Composite silica/alumina and silica/titania materials were prepared by hydrolysis and condensation of the respective metal alkoxides, as described by De Lange [27]. This material is chemically similar to the material that is formed at the interface between the silica and mesoporous layers. As shown in Fig. 5, NH_3 desorbed around $\sim 100^\circ\text{C}$ from the mixed alumina/silica material, while virtually no desorption was observed on the pure silica and silica/titania powders. The desorption peak at $\sim 100^\circ\text{C}$ corresponds well with the adsorption or desorption of NH_3 on or from acidic sites [24,25].

Hence, it appears that the parameters that determine the pervaporation selectivity of microporous silica are both pore size and internal pore chemistry. The presence of acidic sites has a beneficial influence on the water separation properties of the membrane. Most likely, by creating more acidic sites in the selective layer the concentration of the most hydrophilic compound (water) in the membrane is increased, leading to a higher driving force for selective permeation of water. The increased polarity of the micropore wall may

possibly also suppress the flux of the less polar component alcohol.

A separation mechanism based on the hydrophilic nature of the membrane, in accordance with the adsorption–diffusion model, has been extensively studied for zeolite membranes [28]. Using mordenite membranes,

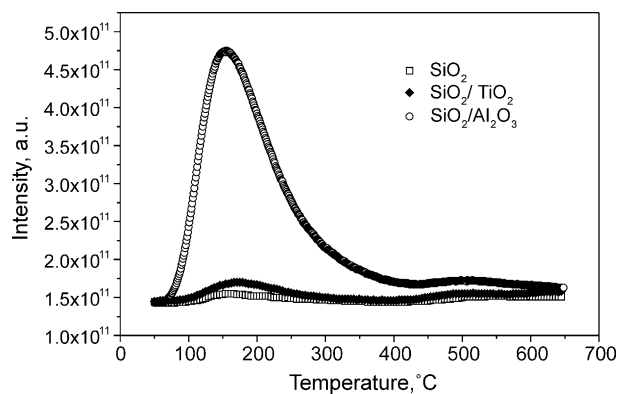


Fig. 5. Temperature programmed desorption of NH_3 from silica, alumina/silica and titania/silica powders.

Casado et al. obtained high separation factors in the pervaporation of ethanol/water mixtures, although a molecular sieving mechanism could be ruled out, since the size of the mordenite channels of $6.5 \times 7.0 \text{ \AA}$ allow an easy entrance of both water and ethanol [28]. Similarly, the differences in activated diffusion rates of water and ethanol did not seem large enough to justify the high separation factors obtained, especially when it was taken into account that the experiments were carried out under conditions where surface adsorption processes exert a considerable influence. Instead, separation was thought to take place primarily due to the hydrophilic character of mordenite. Preferential water adsorption occurred, thereby hindering the passage of ethanol through zeolitic and small non-zeolitic pores. Since the chemical nature of mordenite is roughly similar to the one formed in the interfacial region between γ -alumina and microporous silica, the same explanation may hold here.

4. Conclusions

Microporous silica membranes can be used for separation of water from a wide range of alcohols. Separation occurs primarily due to a molecular sieving effect. However, the chemical nature of the separating layer also plays a pronounced role. The system $\alpha\text{-Al}_2\text{O}_3$ /(anatase) $\text{TiO}_2/\text{SiO}_2$ has an improved chemical stability in comparison with the one containing $\gamma\text{-Al}_2\text{O}_3$ and both systems may be applied in the dewatering of alcohols. This study showed that the chemical nature of the intermediate mesoporous layer material can also play a crucial role in the selectivity of the separation process. The use of γ -alumina as intermediate layer increases the hydrophilicity of the system, promoting adsorption and diffusion of water.

Acknowledgements

This work was financially supported by the European Communities in the framework of the Growth Programme, contract no. G1RD-CT-1999-00076. Dr. J. Xu and Dr. B. Mojet are gratefully acknowledged for performing the TPD experiments.

References

- [1] X. Feng, R.Y.M. Huang, Liquid separation by membrane pervaporation: a review, *Ind. Eng. Chem. Res.* 36 (1997) 1048.
- [2] G.P. Fotou, Y.S. Lin, S.E. Pratsinis, Hydrothermal stability of pure and modified microporous silica membranes, *J. Mater. Sci.* 30 (1995) 2803.
- [3] H. Imai, H. Morimoto, A. Tominaga, H. Hirashima, Structural changes in sol-derived SiO_2 and TiO_2 films by exposure to water vapour, *J. Sol-Gel Sci. Tech.* 10 (1997) 45.
- [4] C.-H. Chang, R. Gopalan, Y.S. Lin, A comparative study on thermal and hydrothermal stability of alumina, titania and zirconia membranes, *J. Membr. Sci.* 91 (1994) 27.
- [5] R.W. van Gemert, F.P. Cuperus, Newly developed ceramic membranes for dehydration and separation of organic mixtures by pervaporation, *J. Membr. Sci.* 105 (1995) 287.
- [6] T. Van Gestel, C. Vandecasteele, A. Buekenhoudt, C. Dotremont, J. Luyten, B. Van der Bruggen, G. Maes, Corrosion properties of alumina and titania NF membranes, *J. Membr. Sci.* 214 (2003) 21.
- [7] T. Van Gestel, C. Vandecasteele, A. Buekenhoudt, C. Dotremont, J. Luyten, R. Leysen, B. Van der Bruggen, G. Maes, Alumina and titania multilayer membranes for nanofiltration: preparation, characterization and chemical stability, *J. Membr. Sci.* 207 (2002) 73.
- [8] J. Sekulić, M.W.J. Luiten, J.E. ten Elshof, N.E. Benes, K. Keizer, Microporous silica and doped silica membrane for alcohol dehydration by pervaporation, *Desalination* 148 (2002) 19.
- [9] J.G. Wijmans, R.W. Baker, The solution diffusion model: a review, *J. Membr. Sci.* 107 (1995) 1.
- [10] F. Lipnizki, G. Trägårdh, Modelling of pervaporation: models to analyze and predict the mass transport in pervaporation, *Separ. Purif. Meth.* 30 (2001) 49.
- [11] T. Bowen, S. Li, R.D. Noble, J.L. Falconer, Driving force for pervaporation through zeolite membranes, *J. Membr. Sci.* 225 (2003) 165.
- [12] A. Heintz, W. Stephan, A generalized solution diffusion-model of the pervaporation process through composite membranes. 2. Concentration polarization, coupled diffusion and the influence of the porous support layer, *J. Membr. Sci.* 89 (1994) 153.
- [13] P. Izák, L. Bartovská, K. Friess, M. Šípek, P. Uchytil, Description of binary liquid mixtures transport through non-porous membrane by modified Maxwell–Stefan equations, *J. Membr. Sci.* 214 (2003) 293.
- [14] X. Ni, X. Sun, D. Ceng, F. Hua, Coupled diffusion of water and ethanol in a polyimide membrane, *Polym. Eng. Sci.* 41 (2001) 1440.
- [15] A.W. Verkerk, P. van Male, M.A.G. Vorstman, J.T.F. Keurentjes, Description of dehydration performance of amorphous silica pervaporation membranes, *J. Membr. Sci.* 193 (2001) 227.
- [16] J.E. ten Elshof, C. Rubio Abadal, J. Sekulić, S.R. Chowdhury, D.H.A. Blank, Transport mechanisms of water and organic solvents through microporous silica in the pervaporation of binary liquids, *Micropor. Mesopor. Mater.* 65 (2003) 197.
- [17] J. Xiao, J. Wei, Diffusion mechanism of hydrocarbons in zeolites, *Chem. Eng. Sci.* 47 (1992) 1123.
- [18] F.F. Lange, Powder processing science and technology for increased reliability, *J. Am. Ceram. Soc.* 72 (1989) 3.
- [19] R.J. van Vuren, B.C. Bonekamp, K. Keizer, R.J.R. Ulhorn, H.J. Veringa, A.J. Burggraaf, Formation of ceramic alumina membranes for gas separation, in: P. Vincenzini (Ed.), *High Tech Ceramics*, Elsevier, Amsterdam, 1987, pp. 2235–2245.
- [20] J. Sekulić, A. Magrasso, J.E. ten Elshof, D.H.A. Blank, Influence of ZrO_2 doping on microstructure and liquid permeability of mesoporous TiO_2 membranes, *Micropor. Mesopor. Mater.* 72 (2004) 49.
- [21] K. Keizer, R.S.A. De Lange, J.H.A. Hekkink, A.J. Burggraaf, Polymeric-silica-based sols for membrane modification applications: Sol-gel synthesis and characterization with SAXS, *J. Non-Cryst. Solids* 191 (1995) 1.
- [22] J. Gmehling, U. Onken, W. Arlt, *Vapor–Liquid Equilibrium Data Collection*, Dechema, Frankfurt, 1981.
- [23] R.M. de Vos, H. Verweij, High-selectivity, high-flux silica membranes for gas separation, *Science* 279 (1998) 1710.
- [24] A. Auroux, R. Monaci, E. Rombi, V. Solinas, A. Sorrentino, E. Santacesaria, Acid sites investigation of simple and mixed oxides by TPD and microcalorimetric techniques, *Thermochim. Acta* 379 (2001) 227.

- [25] M. Sasidharan, S.G. Hegde, R. Kumar, Surface acidity of Al-, Ga- and Fe-silicate analogues of zeolite NCL-1 characterized by FTIR, TPD (NH₃) and catalytic methods, *Micropor. Mesopor. Mater.* 24 (1998) 59.
- [26] <http://srdata.nist.gov/xps>.
- [27] R.S.A. de Lange, Microporous sol-gel derived ceramic membranes for gas separation, PhD Thesis, University of Twente, 1993.
- [28] L. Casado, R. Mallada, C. Téllez, J. Coronas, M. Menéndez, J. Santamaría, Preparation, characterization and pervaporation performance of mordenite membranes, *J. Membr. Sci.* 216 (2003) 135.